Published in final edited form as:
Cell Metab. 2009 September ; 10(3): 208–218. doi:10.1016/j.cmet.2009.07.003.

Nogo-B Receptor stabilizes Niemann-Pick Type C2 protein and regulates intracellular cholesterol trafficking

Kenneth D. Harrison[1], **Robert Qing Miao**[1,2], **Carlos Fernandez-Hernándo**[1], **Yajaira Suárez**[1], **Alberto Dávalos**[1], and **William C. Sessa**[1,3]

[1]Department of Pharmacology and Vascular Biology and Therapeutics Program, Yale University School of Medicine, New Haven, CT 06520.

[2]Departments of Surgery and Pathology, Children's Research Institute, Medical College of Wisconsin, Milwaukee, WI 53226, USA.

Summary

The Nogo-B Receptor (NgBR) is a recently identified receptor for the N-terminus of Reticulon 4B/Nogo-B. Other than its role in binding Nogo-B, little is known about the biology of NgBR. To elucidate a basic cellular role for NgBR, we performed a yeast-2-hybrid screen for interacting proteins using the C-terminal domain as bait and identified Niemann-Pick Type C2 protein (NPC2) as an NgBR-interacting protein. NPC2 protein levels are increased in the presence of NgBR and NgBR enhances NPC2 protein stability. NgBR localizes primarily to the endoplasmic reticulum (ER), and regulates the stability of nascent NPC2. RNAi-mediated disruption of NgBR or genetic deficiency in NgBR leads to a decrease in NPC2 levels, increased intracellular cholesterol accumulation and a loss of sterol sensing, all hallmarks of an NPC2 mutation. These data identify NgBR as an NPC2-interacting protein and provide evidence of a role for NgBR in intracellular cholesterol trafficking.

Introduction

Cholesterol homeostasis is critical for the integrity of numerous cellular functions. A large proportion of intracellular cholesterol is derived from low density lipoprotein receptor (LDL-R) mediated uptake of exogenous cholesterol (Brown and Goldstein, 1986). After LDL-R-mediated internalization, cholesterol is trafficked from endosomes to lysosomes and ultimately delivered to the plasma membrane, endoplasmic reticulum (ER), and to the membranes of other organelles (Ikonen, 2008; Maxfield and Menon, 2006). Specialized membrane proteins localized to the ER serve as sterol sensors and thereby regulate both *de novo* biosynthesis and uptake of cholesterol (Goldstein et al., 2006). The absence of proper regulation of sterol trafficking to the ER results in broad defects in intracellular cholesterol homeostasis.

Studies of a number of congenital disorders of lipid metabolism have provided critical insights into the cell biology of cholesterol trafficking. One disorder of interest is Niemann-Pick Type C disease (NPC), a lysosomal storage disease which results in the intracellular accumulation of cholesterol and defects in sterol regulatory responses, leading to progressive

3**To whom correspondence should be addressed:** Vascular Biology & Therapeutics Program, Amistad Research Building, 10 Amistad Street, Yale University, New Haven, CT 06536. william.sessa@yale.edu.

neurodegeneration and liver failure (Kruth et al., 1986; Liscum and Faust, 1987; Pentchev, 2004). Mutations in either of two genes, *NPC1 or NPC2*, result in the NPC phenotype (Carstea et al., 1997; Loftus et al., 1997; Naureckiene et al., 2000). NPC1 is a polytopic transmembrane protein that resides primarily in late endocytic organelles and contains an intraluminal loop to which cholesterol binds (Infante et al., 2008a; Scott and Ioannou, 2004). NPC2 is a soluble glycoprotein (Naureckiene et al., 2000) that binds cholesterol with nanomolar affinity and is thought to function by transferring cholesterol between membranes (Cheruku et al., 2006; Friedland et al., 2003; Ko et al., 2003). In the absence of NPC1 or NPC2 the efficiency of cholesterol egress from the lysosomal compartment is impaired, the ER does not readily sense LDL-derived cholesterol, and LDL uptake and cholesterol biosynthesis continue unabated (Liscum et al., 1989). These phenotypic similarities have led to the proposal that both genes function in the same pathway (Sleat et al., 2004). The recent development of in vitro assays for measurements of NPC1 and NPC2 sterol transfer has provided insights into the mechanisms by which NPC1 and NPC2 may transfer cholesterol at the endosomal level (Babalola et al., 2007; Infante et al., 2008b). Despite these important advances, however, a paucity of information exists concerning the regulation of NPC2 protein function.

Our group discovered that the reticulon 4B, termed Nogo-B, is highly expressed in the ER and in caveolin-1 enriched microdomains (CEM) in endothelial cells (EC) and vascular smooth muscle cells (VSMCs) (Acevedo et al., 2004). A screen for a receptor for the N-terminal portion of Nogo-B resulted in the characterization of a novel gene product named Nogo-B receptor (NgBR) (Miao et al., 2006). NgBR expression is necessary for Nogo-B-induced chemotaxis and morphogenesis of EC *in vitro*. Other than binding Nogo-B, the basic functions of this gene product are not known.

Here we report that NPC2 is an NgBR-interacting protein as identified in a yeast-2-hybrid screen. The interaction is recapitulated in mammalian cells and co-expression of NgBR with NPC2 enhances NPC2 core protein stability whereas loss of NgBR decreases NPC2 protein levels. In addition, loss of NgBR using siRNA or via gene targeting results in cellular phenotypes reminiscent of NPC disease, including accumulation of free cholesterol and upregulation of LDL uptake consistent with a defect in cholesterol trafficking to the ER. These studies support a role for NgBR as an NPC2-interacting protein and suggest avenues for enhancing NPC2 protein stability and thereby influencing the regulation of intracellular cholesterol trafficking.

Results and Discussion

Evidence of an NgBR-NPC2 interaction

Analysis of the primary sequence of NgBR (Figure S1A) reveals a single C-terminal domain with homology to cis-isoprenyltransferase (cis-IPTase). cis-IPTase domains bind isoprenyl lipids and catalyze the condensation of isopentenyl diphosphate to farnesyl diphosphate to form long-chain polyprenyl diphosphates. Previous studies using partially purified NgBR showed that it lacks cis-IPTase activity (Miao et al., 2006). In order to gain insights into NgBR function, we used the C-terminal domain of NgBR as bait and screened a human heart cDNA expression library in a yeast two-hybrid assay. After several rounds of screening and selection, unique clones were isolated and one of the strongest interactions was seen between the C-terminus of NgBR and NPC2 as measured by alpha-galactosidase secretion (Figures S1B, S1C). These data support the previously detected interaction between NPC2 and human dehydrodolichyl disphosphate synthase (DHDDS, also referred to as HDS, or human cis-isoprenyltransferase; hCIT) (Kharel et al., 2004), the only other mammalian protein characterized thus far with a cis-IPTase domain (Shridas et al., 2003). However, the functional relevance of the DHDDS-NPC2 interaction remains unknown.

The interaction between the cis-IPTase domain in NgBR and full length NPC2 was confirmed in mammalian cells by immunoprecipitation experiments. Transfection of NPC2-myc into CHO cells stably-expressing either vector alone (Vector), NgBR-HA (NgBR), or a deletion mutant of NgBR that lacks the C-terminal cis-IPTase domain (NgBRΔC) followed by immunoprecipitation of NgBR-HA demonstrates a clear interaction between NPC2 and NgBR that is absent in cells expressing NgBRΔC (Figure 1A). We also tested the idea that the previously described interaction between NgBR and the N-terminus of Nogo-B (AmNgB) might influence the NgBR-NPC2 interaction. Addition of recombinant AmNgB to CHO-NgBR cells had no effect on the interaction between NgBR and NPC2, suggesting that NgBR has a distinct subcellular role independent of AmNgB.

Since NPC2 is a secreted glycoprotein, we examined NgBR topology using several approaches. Initially, we cloned the hNPC2 Asn58 glycosylation site in frame at the N- ('N-glyco') and C-termini ('C-glyco') of NgBR (Figure S2A). We also cloned this tag onto a well-characterized peripheral membrane protein, endothelial nitric oxide synthase (eNOS), as a negative control. Expression of the N- and C-glyco mutants of NgBR resulted in mobility shifts by SDS-PAGE that were sensitive to Endoglycosidase H (EndoH) treatment, suggesting that a proportion of these regions of NgBR are luminally oriented. Treatment of both WT and C-glyco eNOS did not show any appreciable differences in mobility (Figure S2B). We further addressed membrane topology of NgBR by limited proteolysis experiments. We cloned a myc epitope tag at the extreme N-terminus of NgBR and analyzed loss of this epitope after trypsin digestion (Figure S2C). In the absence of detergent, the luminal ER chaperone Grp94 is not cleaved to an appreciable extent by trypsin; however, when detergent is present, the membrane is permeabilized and Grp94 is accessible to protease. Analysis of myc and HA (N- and C-termini of NgBR, respectively) shows that a proportion of these epitopes are oriented luminally, as the accessibility of these epitopes to trypsin is enhanced in the presence of detergent. These data suggest that NgBR conforms to a topology different from that suggested by the initial bioinformatic analysis, in that both the N- and C-termini can be arranged with a luminal orientation.

Analysis of the primary sequence of NgBR using the SignalP server (Bendtsen et al, 2004) results in the possibility of either a signal peptide (probability = 0.262) or a signal anchor (an uncleaved signal peptide; probability = 0.718) that consists of amino acids 1–23 from the N-terminus of NgBR. We took two approaches to distinguish between these possibilities. First, we utilized the myc-NgBR-HA construct described above to assess cleavage of the N-terminal 23 amino acids. If any portion of the NgBR N-terminus is cleaved by signal peptidase, then loss of the myc epitope should occur and thus be undetectable. SDS-PAGE analysis of myc-NgBR-HA showed that the myc epitope remains intact, and myc-NgBR-HA migrates with slightly slower mobility than NgBR-HA (Figure S2D), providing evidence of a potential signal anchor motif at the N-terminus of NgBR. In addition, we reasoned if NgBR contains a cleaved signal peptide, then deletion of the N-terminal 23 amino acids should result in a protein which migrates with the same mobility as WT NgBR by SDS-PAGE (Figure S2E). In fact, deletion of this N-terminal region of NgBR resulted in a protein which migrated faster than WT NgBR (Figure S2F), supporting the argument that this region remains intact in WT NgBR and is not a cleaved signal peptide. These data provide evidence that NgBR is not a canonical Type I transmembrane protein as originally predicted by bioinformatics analysis and is atypical in its membrane orientation. Collectively, these data support the conclusion that the C-terminal region of NgBR is necessary for the NgBR-NPC2 interaction in mammalian cells and confirm the yeast two-hybrid results.

While conducting the above co-immunoprecipitation experiments, we observed a significant and reproducible increase in ectopically-expressed NPC2 in CHO-NgBR cells relative to CHO-Vector or CHO-NgBRΔC cells. As the plasmid expressing NPC2 is under the control of a

CMV promoter, a plausible explanation for the increase in NPC2 levels is that NgBR decreases the turnover of NPC2 protein. Indeed, increasing the concentration of NPC2-myc dose-dependently enhanced the levels of NPC2-myc in lysates from CHO-NgBR cells, but not in lysates from cells expressing either vector alone or NgBRΔC (Figure 1B). Moreover, levels of NPC2 secreted into the media of CHO-NgBR were greatly enhanced compared to CHO cells expressing vector alone (Figure 1C). In order to examine possible effects of NgBR on NPC2 protein stability, we performed pulse-chase experiments by expressing NPC2 in the absence or presence of NgBR. The $t_{1/2}$ of NPC2 in the absence of NgBR was 3.5hrs, while the $t_{1/2}$ of NPC2 in the presence of NgBR was 5.1hrs, reflecting an almost 50% increase in NPC2 stability (Figure 1D).

The preceding experiments were performed in a heterologous system in which both NgBR and NPC2 were ectopically expressed. In order to confirm these results in cells that express high endogenous levels of both NgBR and NPC2, we used HepG2 cells (a hepatocarcinoma cell line) and EA.hy926 cells (EA.hy; a hybridoma cell line created by fusion of HUVEC and A549) and employed an RNAi-mediated approach to decrease NgBR expression. siRNA directed against NgBR reduces NgBR levels by 80–90% (Figure 1E) and the loss of NgBR reduces endogenous NPC2 expression in both cell lines (the loss of NgBR reduces NPC2 levels by 35.5% +/−and 49.3%+/−12.2 in HepG2 and EA.hy926 cells, respectively, n=5 independent experiments). In order to assess whether the loss of NgBR influenced the levels of another endosomal/lysosomal glycoprotein, we also probed for another soluble lysosomal glycoprotein, cathepsin D. Levels of cathepsin D remain unaffected by loss of NgBR, suggesting a specific effect of NgBR expression on NPC2 stability. In order to gain insight into the mechanism by which NgBR-regulates NPC2 stability, we tested the proteasomal dependence of NPC2 degradation. Treatment of cells with proteasome inhibitors, MG132 or lactacystin, prevented the loss of NPC2 following NgBR knockdown (Figure 1F). Collectively, these data suggest that NgBR expression is necessary for NPC2 stability.

The interaction between NgBR and NPC2 occurs in a pre-lysosomal compartment

In order to gain further insights into the interaction between NgBR and NPC2, we assessed NgBR and NPC2 colocalization by immunofluorescence. Detection of endogenous NPC2 by immunofluorescence is dependent on the usage of Bouin's fixative for reliable detection (Zhang et al., 2003). Detection of NgBR is limited to HA-tagged NgBR using antibodies directed against the HA epitope in order to maintain compatibility with Bouin’s fixation. Endogenous NPC2 has been reported previously to localize to lysosomal, late endosomal, and trans-Golgi network (TGN) compartments (Berger et al., 2007; Naureckiene et al., 2000; Zhang et al., 2003). NgBR-HA colocalizes with NPC2 both in punctuate structures and in a diffuse perinuclear compartment (Figure 2A). In agreement with previous reports, endogenous NPC2 colocalizes to a large extent with cathepsin D (Figure 2B). NgBR-HA, however, does not colocalize with cathepsin D, suggesting an alternate subcellular compartment in which the NgBR-NPC2 interaction takes place (Figure 2C). We tested a variety of organelle markers for colocalization with NgBR-HA, and determined that ER markers such as protein disulfide isomerase (PDI) and calnexin exhibit the highest degree of colocalization (Figure 2D). NPC2 contains a canonical signal peptide and is a soluble luminal glycoprotein, thus a fraction of NPC2 should be present within the ER lumen during its biosynthesis. In order to ascertain whether any degree of similar compartmentalization between NgBR-HA and NPC2 exists at steady-state, we co-labeled cells for NPC2 and PDI. NPC2 partially colocalizes with PDI, suggesting the ER is one compartment in which the NgBR and NPC2 interaction might occur (Figure 2E).

We sought an independent, biochemical approach to more rigorously address the localization of NgBR in the context of these studies. Given the enrichment of NgBR in the ER compartment,

we utilized a recently described approach to purify ER membranes from cultured cells using a continuous iodixanol gradient separation of ER and lysosomal membranes (Radhakrishnan et al., 2008). As seen in Figure 3A, the ER marker calnexin predominantly localizes to the denser regions of the iodixanol gradient (designated as region (2) in Figure 3), whereas the lysosomal marker Cathepsin D is almost exclusively present in the floating membrane layer (designated as (1) in Figure 3). NPC2 again cofractionated with Cathepsin D as expected, however, the levels of endogenous NgBR were beyond detection due to dilution of the fractions. In order to assess the fractionation of NgBR, we ectopically expressed a FLAG-tagged NgBR cDNA and determined that NgBR shows a pattern of fractionation similar to calnexin (Figure 3B) and the expression of NgBR enhanced the levels of endogenous NPC2 in regions 1 and 2 of the gradient. Since we could not detect NPC2 in region 2 of the fractions in the absence of ectopic NgBR expression (Figure 3A), yet could detect NPC2 in these regions of the gradient in the presence of NgBR, these data suggest that forced expression of NgBR may result in the appearance of NPC2 in the ER to a more appreciable extent. We tested this hypothesis by performing immunofluoresence in cells expressing either full-length NgBR or the C-terminal truncation mutant of NgBR that does not bind NPC2. In cells transfected with a control plasmid, NPC2 displays a punctate pattern that does not colocalize with the ER marker PDI (Figure 3C). In cells overexpressing WT NgBR, NPC2 exhibits a more reticular distribution coupled with the same punctate pattern seen in control transfected cells (Figure 3D). This distribution of NPC2 is dependent on the presence of the C-terminal region of NgBR, as cells expressing NgBRΔC display a pattern of NPC2 distribution similar to control (Figure 3E). These results are unlikely to be explained by non-specific effects of overexpression, as transfection of the protein palmitoyltransferase DHHC3 (Fernandez-Hernando et al, 2006) also results in a pattern of NPC2 distribution similar to control plasmid transfected cells (Figure 3F). These data bolster the idea that NgBR functions to stabilize NPC2 during transit in the ER.

Our previous data showing that NPC2 protein levels are enhanced in the presence of NgBR allowed for further biochemical approaches to test this hypothesis. We tested the stage at which the NgBR-NPC2 interaction occurs using several approaches. We blocked NPC2 glycosylation with tunicamycin in the presence or absence of NgBR expression followed by cell lysis and immunoblotting for NPC2. Surprisingly, expression of NgBR increases NPC2 core protein levels in the presence of tunicamycin (Figure 4A), suggesting that NgBR functions to stabilize nascent NPC2. In order to further address the stage at which NgBR affects NPC2, we mutated Asn39 (of mature NPC2) to Gln ($NPC2^{N58Q}$). $NPC2^{N58Q}$ has been shown previously to prevent proper targeting of NPC2 to the lysosome, presumably by interfering with a mannose-6-phosphate receptor (MPR)-dependent mechanism (Chikh et al., 2004; Liou et al., 2006). $NPC2^{N58Q}$ levels are also higher in the presence of NgBR (Figure 4B), again suggesting a role for NgBR in stabilizing an extra-lysosomal form of NPC2. We next tested the possibility that NgBR might influence lysosomal NPC2 levels in a more direct manner. As has been shown previously, NPC2 is a secreted glycoprotein and conditioned medium from cells expressing NPC2 can functionally rescue cholesterol trafficking defects in cells deficient in endogenous NPC2 expression, providing strong evidence for internalization of exogenous NPC2 into the lysosomal compartment (Naureckiene et al., 2000; Ko et al., 2003). We collected and concentrated conditioned medium from CHO cells transfected with myc-tagged NPC2 and then incubated cells treated with Ctrl RNAi or NgBR RNAi for the indicated times (Figure 4C). Rather than result in loss of lysosomal NPC2 stability, downregulation of NgBR in this context seemed to slightly enhance NPC2 uptake. This effect was not seen in control experiments in which U18666A (a drug that induces cholesterol sequestration in late endosomes/lysosomes and mimics an NPC phenotype) was used as a control for accumulation in the lysosomal compartment (Figure 4C). This offers the interesting possibility that loss of NPC2 at the level of the ER may activate mechanisms to augment the uptake and storage of lysosomal NPC2. Finally, to test whether blockade of ER-Golgi trafficking with brefeldin A

(BFA) would influence NPC2 stability, control or NgBR expressing CHO cells were treated with different concentrations of BFA. Interestingly, BFA further enhanced the stabilizing effect provided by NgBR (Figure 4D). Coupled with the immunofluorescence results, these data provide evidence of an interaction between NgBR and NPC2 occurring in a pre-lysosomal compartment.

Evidence of a role for NgBR in intracellular cholesterol trafficking

Due to the accumulation of cholesterol that occurs with loss of NPC2 expression, we sought to determine whether a similar phenotype exists with loss of NgBR. In order to examine whether reduction of endogenous NgBR impacts cholesterol trafficking, HepG2 cells were treated with control siRNA (Ctrl RNAi), NgBR siRNA (NgBR RNAi) or U18666A (as a positive control to induce an NPC phenotype), stained with filipin and free cholesterol pools were examined by fluorescence microscopy. NgBR RNAi-treated cells exhibit increased free cholesterol levels as shown by the higher intensity of filipin fluorescence relative to Ctrl RNAi-treated cells (Figure 5A). These data suggest that NgBR influences cellular cholesterol trafficking and that the lack of NgBR expression results in accumulation of free cholesterol. In addition, we derived fibroblasts (MEFs) from WT and $NgBR^{+/-}$ ES cells and assessed free cholesterol levels by filipin staining. $NgBR^{+/-}$ MEFs exhibit an increased level of filipin fluorescence intensity relative to WT MEFs (Figure 5B), providing genetic support for a role for NgBR in intracellular cholesterol trafficking. To address the possibility that Nogo-B may regulate these NgBR-dependent defects in cholesterol trafficking, we stained Nogo-A/B double knockout fibroblasts with filipin. No appreciable differences in free cholesterol levels were observed in Nogo-A/B knockout cells (Figure S3), again suggesting that the NgBR-NPC2 interaction is independent of Nogo-A or –B.

The siRNA sequence used in the preceding experiments targets the 3' untranslated region (UTR) of the NgBR transcript, an approach that allows for the rescue of cells by expression of NgBR lacking the 3' UTR (Miao et al., 2006). We exploited these sequence differences through introduction of an RNAi-resistant NgBR construct in cells treated with NgBR RNAi. Transduction of cells with adenoviral NgBR (Ad-NgBR) alleviates the increase in free cholesterol and the reduction in NPC2 levels seen after treatment with NgBR RNAi (Figure 5C). In order to address the mechanism by which this accumulation of cholesterol occurs, we treated cells with diminished NgBR with conditioned media collected from cells overexpressing secreted NPC2. Exogenous NPC2, but not mock transfected conditioned media nor media collected from cells expressing $NPC2^{N58Q}$, rescued the increase in free cholesterol seen with NgBR RNAi treatment (Figure 5D), suggesting that this effect is NPC2-dependent. Efforts to understand the basis of NPC disease have led to the discovery that the NPC phenotype is in part due to defects in sterol trafficking to sites of oxysterol biosynthesis (Frolov et al., 2003; Zhang et al., 2008). To address the question of whether NgBR might function in a similar manner, we incubated NgBR RNAi-treated cells with 25-hydroxycholesterol (25-HC), and again stained with filipin. Cholesterol accumulation seen after NgBR RNAi treatment was alleviated by incubation with 25-HC (Figure 5E) as shown previously for cells deficient in NPC2 function by Ory and colleagues (Frolov et al., 2003), lending further credence to the hypothesis that similar sterol trafficking defects occur with loss of NgBR or NPC2.

NgBR is important for proper maintenance of sterol sensing

Fibroblasts from Niemann-Pick Type C patients exhibit defects in sterol sensing as a result of the cholesterol accumulation that occurs upstream of the ER-resident sterol sensing machinery (Liscum and Faust, 1987). In order to determine whether NgBR-dependent sterol trafficking defects lead to dysregulation of sterol sensing in a manner reminiscent of NPC2 disease, we reduced NgBR levels with RNAi and assessed sterol responsiveness. Initially, we assessed the relatively acute suppression of SREBP cleavage that occurs with addition of exogenous LDL

to cells incubated in the absence of lipoproteins in the media. As seen in Figure 6A, induction of SREBP cleavage occurs when cells are cultured in the absence of lipoproteins (lipoprotein deficient serum, LPDS). This cleavage is partially suppressed when exogenous LDL is added to the medium (Figure 6A, +nLDL). However, knockdown of NgBR or treatment with U18666A abrogated this suppressive effect of LDL on SREBP cleavage. Seeking to determine the functional consequence of this dysregulation, HepG2 cells were treated with Ctrl RNAi or NgBR RNAi, the biosynthetic pool of cholesterol labeled using [^{14}C]-acetate and *de novo* cholesterol biosynthesis measured. Knockdown of NgBR expression leads to an enhanced rate of cholesterol synthesis relative to Ctrl RNAi-treated cells (Figure 6B). Next, we assessed another index of sterol responsiveness by measuring the specific uptake of DiI-labeled LDL. EA.hy cells treated with Ctrl RNAi exhibit a dose-dependent decrease in LDL uptake when incubated for 48hrs in the presence of increasing concentrations of nLDL (data not shown). However, loss of NgBR expression leads to diminished sterol sensitivity, as DiI-LDL uptake is increased upon NgBR knockdown despite pre-incubation of cells with nLDL prior to DiI-LDL treatment (Figure 6C). Moreover, this increase in uptake is mirrored by an increase in cell surface binding of LDL (Figure 6D), suggesting that more LDL-R is present at the cell surface in the absence of NgBR expression. Indeed, HepG2 cells treated with NgBR siRNA exhibit increased levels of total and surface LDL-R (Figure S4B, and Figure 6E, respectively).

In order to determine the relative specificity of the effects described above, we performed rescue experiments with an NgBR cDNA construct lacking the RNAi target sequence. Treatment of HepG2 with NgBR RNAi leads to ~90% loss of NgBR expression, while RNAi against NgBR in cells stably expressing the coding sequence alone leads to loss of endogenous NgBR (E) but not transfected NgBR (R) (Figure 6F). Indeed, cells stably expressing transfected NgBR did not show any appreciable increase in LDL-R expression after siRNA treatment (Figure S4C, Figure 6G; total and surface LDL-R, respectively), proving the specificity of the RNAi effects seen in prior experiments. We also treated cells with 25-HC as in the filipin staining experiments in order to further address the mechanistic basis for the increase in LDL-R levels. Incubation of EA.hy cells with 25-HC results in a dramatic decrease in both total (Figure S4D) and surface (Figure 6H) LDL-R expression in cells treated with NgBR RNAi. Next, we performed analogous experiments in primary cultures of human skin fibroblasts since the above experiments were performed in immortalized cell lines. Fibroblasts treated with NgBR RNAi again exhibited increased intracellular cholesterol accumulation (Figure S5A) and diminished suppression of SREBP cleavage in the presence of LDL-cholesterol (Figure S5B), providing support for a role for NgBR in cholesterol homeostasis. Thus, the loss of NgBR leads to dysregulation of sterol homeostasis consistent with the accumulation of free cholesterol as occurs in NPC2 disease.

In summary, we have identified a function for NgBR as an NPC2 binding partner that regulates NPC2 stability/turnover. Our data suggest that the NgBR cis-IPTase homology domain is crucial for its interaction with NPC2 in yeast and heterologous mammalian expression systems. These data are particularly compelling in light of the previously described interaction between NPC2 and the cis-IPTase domain of DHDDS. Future efforts will seek to define a possible relationship between NPC2, NgBR and DHDDS.

Although it is well appreciated that the functional relationship between NPC1 and NPC2 is critical for cholesterol trafficking, our data provide compelling evidence for an unappreciated mode of NPC2 regulation via this newly described interaction. Interestingly, NgBR partially colocalizes with NPC2 in the ER and enhances the levels of nascent NPC2 protein. Our results are in agreement with numerous studies which have shown NPC2 to be primarily localized to a lysosomal compartment at steady-state; however, our data suggests that an additional level of regulation has evolved to ensure stability of NPC2 at its earliest steps of entry into the secretory pathway. The idea that a unique chaperone function may be conferred by non-

canonical binding events within the ER is not unprecedented and has been suggested for other proteins (Ju et al., 2008).

The effects of NgBR on NPC2 described herein appear to be independent of the only other described binding partner for NgBR, Nogo-B. Loss of NgBR genetically or using siRNA leads to cholesterol accumulation which, in turn, results in defects in ER sterol sensing, both of which are phenotypic hallmarks of mutations in NPC2. Thus, these data reveal insights into NPC2 trafficking, protein stability, and cholesterol homeostasis and raise the possibility that loss of function mutations in NgBR may promote defects in cholesterol metabolism.

Experimental Procedures

Description of methods pertaining to Yeast-2-Hybrid analysis, cell culture, immunoprecipitation and western blot analysis, cell fractionation, and protease protection assays are presented within Supplementary Experimental Procedures.

Materials

Express [^{35}S} protein labeling mix (NEG-072) was from Perkin Elmer; MG132, lactacystin, U18666A, and brefeldin A were purchased from EMD Biosciences; filipin and Bouin's fixative were from Sigma; 25-hydroxycholesterol was purchased from Steraloids, Inc.; EndoH was from New England Biolabs, The origin of other chemicals and antibodies is described within Experimental Procedures. cDNA constructs are described within Supplementary Experimental Procedures.

Pulse-Chase Analysis

Pulse-Chase studies were performed essentially as described (Liu et al., 1995). Briefly, CHO cells stably expressing either vector alone or full-length NgBR were cultured in 60mm plates and transfected with NPC2-myc at 80% confluency. 24 hours post-transfection, cells were starved in methionine/cysteine-free DMEM + 5% dialyzed FCS for 3 hours at 37 degrees. Labeling was performed for 1 hour at 37 degrees with 200μCi of Express labeling mix (Perkin-Elmer) added to each plate. After 1 hour of labeling, medium supplemented with 2mM methionine and cysteine was added for the designated times, after which cells were lysed and lysates prepared for immunoprecipitation with anti-myc antibodies.

Filipin staining and Immunofluorescence

For detection of intracellular free cholesterol, cells were fixed in 4% PFA at RT for 10 minutes, followed by permeabilization in 0.1% Triton X-100 for 5 minutes at RT. Cells were then incubated with filipin (Sigma, diluted from a stock concentration of 25mg/ml in DMSO to 50ug/ml final concentration in PBS) for 30 minutes at RT. As a positive control for induction of cholesterol accumulation, cells were incubated in DMEM + 10% FBS and treated for 8 hours with 1μM U18666A (EMD Biosciences) prior to fixation. Relative intensity of filipin staining was quantified by calculating average pixel intensity using Adobe Photoshop according to the equation: average filipin intensity = total intensity above low threshold/number of pixels above low threshold (Pipalia et al., 2006). For immunofluorescence, HeLa cells were transfected with pcDNA3-NgBR-HA and fixed with Bouin's fixative for 1 hour at RT. Fixation was followed by permeabilization with 0.1% Triton X-100 for 5 minutes at RT. Cells were blocked in 5% BSA for 30 minutes at RT, and incubated overnight with the following antibodies diluted in 5% BSA: anti-HA (Roche) 1:1000, anti-NPC2 H−125 (Santa Cruz) 1:200, anti-PDI (BD Biosciences) 1:500, anti-Cathepsin D (Santa Cruz) 1:200. Primary antibody incubation was followed by incubation with Alexa-Fluor 488 (1:500), Alexa-Fluor 594 (1:500), or Alexa-Fluor 647 (1:500) conjugated secondary antibodies for 1 hour at RT. Images were captured with a Leica TCS SP5 Spectral Confocal Microscope.

Cholesterol Biosynthesis

Metabolic labeling and analysis of cholesterol biosynthesis was performed as previously described (Fernandez et al., 2002). Briefly, HepG2 cells (6×10^6) were cultured in DMEM + 10% LPDS for 48 hours followed by addition of nLDL for 4 hours, upon which 40μCi [2-^{14}C]acetate used added to the medium of each plate and incubated for 12 hours in order to label the biosynthetic pool of sterol. At the end of the incubation period, cells were washed with ice-cold PBS and resuspended in 0.5ml of 10% (v/v) KOH. [^{3}H]-cholesterol was added as an internal standard. After chloroform:methanol extraction (2:1, v/v), the lipid extract was further subfractionated into saponifiable and nonsaponifiable fractions. The nonsaponifiable fraction was resuspended in hexane and separated by HPLC using a reverse-phase HPLC with a Luna 5um pore size C_{18} column (250mm × 4.60mm; Phenomenex).

LDL uptake

Native plasma LDL was isolated by preparative sequential ultracentrifugation of pooled normolipidemic sera from humans after an overnight fast as described (Calvo et al., 1998). Labeling of LDL with the fluorescence probe 1,1'-diotadecyl-3-3-3'-3'-tetramethylindocarbocyanine perchlorate (DiI) was carried out according to published methods (Via and Smith, 1986). HepG2 or EA.hy926 cells were cultured in 45% OPTI-MEM / 45% DMEM + 10% fetal bovine lipoprotein-deficient serum (Intracel, Inc.) with or without addition of native LDL and containing either Ctrl RNAi or NgBR RNAi for 48 hours prior to addition of 20ug/ml DiI-labeled LDL for a 2 hour incubation period to measure uptake. In order to assess specific uptake of DiI-LDL, control cells were incubated with a 40-fold excess of unlabeled nLDL and uptake values from these cells were subtracted from experimental samples.

LDL-R expression by FACS

HepG2 cells or EA.hy926 cells were seeded in 60mm plates at 30% confluency. After 24 hours of culture, cells were washed twice with PBS and media was replaced with OPTI-MEM containing oligofectamine (Invitrogen) and 10nM siRNA (final concentration) at a 10:1 ratio (oligofectamine:siRNA). siRNAs used in this study were designed using BIOPREDsi (http://www.biopredsi.org) and purchased from Qiagen. The siRNA sequences are: Ctrl RNAi (AllStars Neg. Ctrl siRNA, Qiagen), NgBR RNAi (5'-AAGGAAATACATAGACCTACA-3'). After 48 hours of incubation with siRNA, cells were washed with PBS, trypsinized, washed once in growth medium and resuspended in blocking buffer (1% BSA + 1% normal goat serum in PBS) at a concentration of 10^7 cells/ml. For surface labeling, cells were incubated in blocking buffer for 10 minutes at RT followed by 5 minutes on ice. 100ul of cells (10^6 cells) were incubated on ice with 1.5ug of LDL-R primary antibody (LDL-R C7, Santa Cruz) for 45 minutes. 1.5ug of mIgG2b (Santa Cruz) was used as a control. Following incubation with primary antibody, cells were washed 2 times with blocking buffer and incubated with FITC-conjugated goat anti-mouse secondary antibody for 30 minutes on ice. Cells were again washed twice with blocking buffer and resuspended in PBS. For total LDL-R analysis, cells were fixed with 4% paraformaldehyde immediately after removal from the plate for 15 minutes at room temperature. After 2 washes with blocking buffer, cells were permeabilized with 0.1% Triton X-f100 for 15 minutes at room temperature and again washed 2 times with blocking buffer. After the permeabilization step, cells were stained in an identical manner as presented above for surface-labeled cells. Flow cytometry was performed using a BD FACsort cell sorter. Data are presented as described in the figure legend.

Statistical Analyses

Data are expressed as mean ± S.E. Statistical comparisons between groups were performed using Student's t test or analysis of variance (ANOVA) using Graphpad Software (La Jolla, CA). Significant differences are indicated in the figures.

Acknowledgements

We thank Matthew Scott (Stanford Univ.) for the gift of the NPC2-myc construct, Miguel Lasuncion (Hospital Ramon y Cajal) for nLDL, DiI-LDL and assistance with cholesterol synthesis experiments, Levente Jozsef for deriving Nogo KO embryonic fibroblasts and Zhengrong Hao and Roger Babbitt for excellent technical assistance. This work was supported by grants R01 HL64793, R01 HL61371, R01 HL57665 and P01 Hl70295 from the National Institutes of Health to W.C. Sessa, a Pre-doctoral fellowship from the American Heart Association to K.D. Harrison, a Scientist Development Grant from American Heart Association (to C. Fernández-Hernando, R.Q. Miao and Y.Suárez), and a Programme 3+3 Fellowship from the Centro Nacional de Investigaciones Cardiovasculares (CNIC) (to Y. Suárez). A. Dávalos is recipient of a postdoctoral fellowship from Instituto de Salud Carlos III, Spain.

References

Acevedo L, Yu J, Erdjument-Bromage H, Miao R, Kim J, Fulton D, Tempst P, Strittmatter S, Sessa W. A new role for Nogo as a regulator of vascular remodeling. Nat. Med 2004;10:382–388. [PubMed: 15034570]

Babalola J, Wendeler M, Breiden B, Arenz C, Schwarzmann G, Locatelli-Hoops S, Sandhoff K. Development of an assay for the intermembrane transfer of cholesterol by Niemann-Pick C2 protein. Biol. Chem 2007;388:617–626. [PubMed: 17552909]

Bendtsen J, Nielsen H, von Heijne G, Brunak S. Improved prediction of signal peptides: SignalP 3.0. J. Mol. Biol 2004;340:783–795. [PubMed: 15223320]

Berger A, Salazar G, Styers M, Newell-Litwa K, Werner E, Maue R, Corbett A, Faundez V. The subcellular localization of the Niemann-Pick Type C proteins depends on the adaptor complex AP-3. J.Cell Sci 2007;120:3640–3652. [PubMed: 17895371]

Brown M, Goldstein J. A receptor-mediated pathway for cholesterol homeostasis. Science 1986;232:34–47. [PubMed: 3513311]

Calvo D, Gomez-Coronado D, Suarez Y, Lasuncion M, Vega M. Human CD36 is a high affinity receptor for the native lipoproteins HDL, LDL, and VLDL. J Lipid Res 1998;39:777–788. [PubMed: 9555943]

Carstea E, Morris J, Coleman K, Loftus S, Zhang D, Cummings C, Gu J, Rosenfeld M, Pavan W, Krizman D, et al. Niemann-Pick C1 disease gene: homology to mediators of cholesterol homeostasis. Science 1997;277:228–231. [PubMed: 9211849]

Cheruku S, Xu Z, Dutia R, Lobel P, Storch J. Mechanism of cholesterol transfer from the Niemann-Pick type C2 protein to model membranes supports a role in lysosomal cholesterol transport. J.Biol. Chem 2006;281:31594–31604. [PubMed: 16606609]

Chikh K, Vey S, Simonot C, Vanier M, Millat G. Niemann-Pick type C disease: importance of N-glycosylation sites for function and cellular location of the NPC2 protein. Mol. Genet. and Metab 2004;83:220–230. [PubMed: 15542393]

Fernandez C, Suarez Y, Ferruelo A, Gomez-Coronado D, Lasuncion M. Inhibition of cholesterol biosynthesis by Delta22-unsaturated phytosterols via competitive inhibition of sterol Delta24-reductase in mammalian cells. Biochem. J 2002;366:109–119. [PubMed: 12162789]

Fernandez-Hernando C, Fukata M, Bernatchez P, Fukata Y, Lin M, Bredt D, Sessa W. Identification of Golgi-localized acyl transferases that palmitoylate and regulate endothelial nitric oxide synthase. J. Cell Biol 2006;174:369–377. [PubMed: 16864653]

Friedland N, Liou H-L, Lobel P, Stock A. Structure of a cholesterol-binding protein deficient in Niemann-Pick type C2 disease. Proc. Natl. Acad. Sci. U S A 2003;100:2512–2517. [PubMed: 12591954]

Frolov A, Zielinski S, Crowley J, Dudley-Rucker N, Schaffer J, Ory D. NPC1 and NPC2 regulate cellular cholesterol homeostasis through generation of low density lipoprotein-derived oxysterols. J. Biol. Chem 2003;278:25517–25525. [PubMed: 12719428]

Gelsthorpe M, Baumann N, Millard E, Gale S, Langmade S, Schaffer J, Ory D. NPC1 I1061T mutant encodes a functional protein that is selected for ER-associated degradation due to protein misfolding. J. Biol. Chem 2008;283:8229–8236. [PubMed: 18216017]

Goldstein J, Debose-Boyd R, Brown M. Protein sensors for membrane sterols. Cell 2006;124:35–46. [PubMed: 16413480]

Hua X, Sakai J, Ho Y, Goldstein J, Brown M. Hairpin orientation of sterol regulatory element-binding protein-2 in cell membranes as determined by protease protection. J. Biol. Chem 1995;270:29422–29427. [PubMed: 7493979]

Ikonen E. Cellular cholesterol trafficking and compartmentalization. Nat. Rev. Mol. Cell Biol 2008;9:125–138. [PubMed: 18216769]

Infante R, Radhakrishnan A, Abi-Mosleh L, Kinch L, Wang M, Grishin N, Goldstein J, Brown M. Purified NPC1 protein: II. Localization of sterol binding to a 240-amino acid soluble luminal loop. J. Biol. Chem 2008;283:1064–1075. [PubMed: 17989072]

Infante R, Abi-Mosleh L, Radhakrishnan A, Dale J, Brown M, Goldstein J. Purified NPC1 protein. I. Binding of cholesterol and oxysterols to a 1278-amino acid membrane protein. J. Biol. Chem 283:1052–1063. [PubMed: 17989073]

Infante R, Wang M, Radhakrishnan A, Kwon H, Brown M, Goldstein J. NPC2 facilitates bidirectional transfer of cholesterol between NPC1 and lipid bilayers, a step in cholesterol egress from lysosomes. Proc. Natl. Acad. Sci 2008;105:15287–15292. [PubMed: 18772377]

Ju T, Aryal R, Stowell S, Cummings R. Regulation of protein O-glycosylation by the endoplasmic reticulum localized molecular chaperone Cosmc. J. Cell Biol 2008;182:531–542. [PubMed: 18695044]

Kharel Y, Takahashi S, Yamashita S, Koyama T. In vivo interaction between the human dehydrodolichyl diphosphate synthase and the Niemann-Pick C2 protein revealed by a yeast two-hybrid system. Biochem. Biophys. Res. Comm 2004;318:198–203. [PubMed: 15110773]

Ko D, Binkley J, Sidow A, Scott M. The integrity of a cholesterol-binding pocket in Niemann-Pick C2 protein is necessary to control lysosome cholesterol levels. Proc. Natl. Acad. Sci. U S A 2003;100:2518–2525. [PubMed: 12591949]

Kruth H, Comly M, Butler J, Vanier M, Fink J, Wenger D, Patel S, Pentchev P. Type C Niemann-Pick disease. Abnormal metabolism of low density lipoprotein in homozygous and heterozygous fibroblasts. J. Biol. Chem 1986;261:16769–16774. [PubMed: 3782141]

Liou H-L, Dixit S, Xu S, Tint G, Stock A, Lobel P. NPC2, the protein deficient in Niemann-Pick C2 disease, consists of multiple glycoforms that bind a variety of sterols. J. Biol. Chem 2006;281:36710–36723. [PubMed: 17018531]

Liscum L, Faust J. Low density lipoprotein (LDL)-mediated suppression of cholesterol synthesis and LDL uptake is defective in Niemann-Pick type C fibroblasts. J. Biol. Chem 1987;262:17002–17008. [PubMed: 3680287]

Liscum L, Ruggiero R, Faust J. The intracellular transport of low density lipoprotein-derived cholesterol is defective in Niemann-Pick type C fibroblasts. J.Cell Biol 1989;108:1625–1636. [PubMed: 2715172]

Liu J, Garcia-Cardena G, Sessa W. Biosynthesis and palmitoylation of endothelial nitric oxide synthase: mutagenesis of palmitoylation sites, cysteines-15 and/or -26, argues against depalmitoylation-induced translocation of the enzyme. Biochemistry 1995;34:12333–12340. [PubMed: 7547976]

Loftus S, Morris J, Carstea E, Gu J, Cummings C, Brown A, Ellison J, Ohno K, Rosenfeld M, Tagle D, et al. Murine model of Niemann-Pick C disease: mutation in a cholesterol homeostasis gene. Science 1997;277:232–235. [PubMed: 9211850]

Maxfield F, Menon A. Intracellular sterol transport and distribution. Curr. Opin. Cell Biol 2006;18:379–385. [PubMed: 16806879]

Miao R, Gao Y, Harrison K, Prendergast J, Acevedo L, Yu J, Hu F, Strittmatter S, Sessa W. Identification of a receptor necessary for Nogo-B stimulated chemotaxis and morphogenesis of endothelial cells. Proc. Natl. Acad. Sci. U S A 2006;103:10997–11002. [PubMed: 16835300]

Naureckiene S, Sleat D, Lackland H, Fensom A, Vanier M, Wattiaux R, Jadot M, Lobel P. Identification of HE1 as the second gene of Niemann-Pick C disease. Science 2000;290:2298–2301. [PubMed: 11125141]

Pentchev P. Niemann-Pick C research from mouse to gene. Biochim. Biophys Acta 2004;1685:3–7. [PubMed: 15465420]

Pipalia N, Huang A, Ralph H, Rujoi M, Maxfield F. Automated microscopy screening for compounds that partially revert cholesterol accumulation in Niemann-Pick C cells. J. Lipid Res 2006;47:284–301. [PubMed: 16288097]

Radhakrishnan A, Goldstein J, McDonald J, Brown M. Switch-like control of SREBP-2 transport triggered by small changes in ER cholesterol: a delicate balance. Cell Metab 2008;8:512–521. [PubMed: 19041766]

Scott C, Ioannou Y. The NPC1 protein: structure implies function. Biochim. Biophys. Acta 2004;1685:8–13. [PubMed: 15465421]

Shridas P, Rush J, Waechter C. Identification and characterization of a cDNA encoding a long-chain cis-isoprenyltranferase involved in dolichyl monophosphate biosynthesis in the ER of brain cells. Biochem. Biophys. Res. Commun 2003;312:1349–1356. [PubMed: 14652022]

Sleat D, Wiseman J, El-Banna M, Price S, Verot L, Shen M, Tint G, Vanier M, Walkley S, Lobel P. Genetic evidence for nonredundant functional coope rativity between NPC1 and NPC2 in lipid transport. Proc. Natl. Acad. Sci. U S A 2004;101:5886–5891. [PubMed: 15071184]

Via D, Smith L. Fluorescent labeling of lipoproteins. Methods Enzymol 1986;129:848–857. [PubMed: 3724556]

Zhang J, Coleman T, Langmade S, Scherrer D, Lane L, Lanier M, Feng C, Sands M, Schaffer J, Semenkovich C, Ory D. Niemann-Pick C1 protects against atherosclerosis in mice via regulation of macrophage intracellular cholesterol trafficking. J. Clin. Invest 2008;118:2281–2290. [PubMed: 18483620]

Zhang M, Sun M, Dwyer N, Comly M, Patel S, Sundaram R, Hanover J, Blanchette-Mackie E. Differential trafficking of the Niemann-Pick C1 and 2 proteins highlights distinct roles in late endocytic lipid trafficking. Acta Paediatr. Suppl 2003;92:63–73. [PubMed: 14989468]

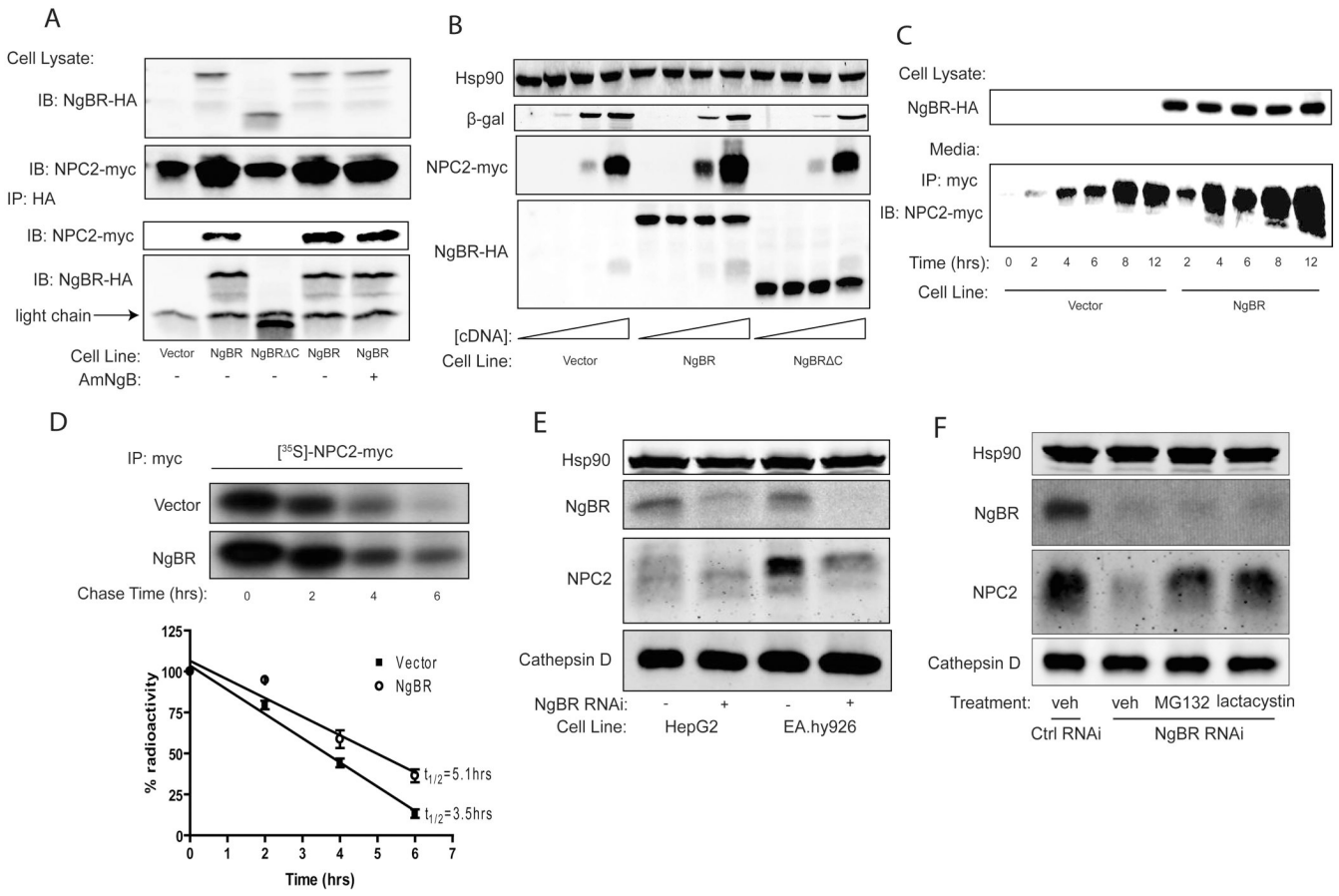

Figure 1. NgBR interacts with and stabilizes NPC2

(A) NgBR interacts with NPC2 in mammalian cells. CHO cell lines stably expressing either vector alone (Vector), HA-tagged, full-length NgBR (NgBR), or an HA-tagged, truncated form of NgBR lacking the C-terminal 158 amino acids (NgBRΔC) were transfected with myc-tagged NPC2. HA-tagged proteins were immunoprecipitated from lysates and subjected to Western blot analysis using anti-myc and anti-HA antibodies. (B) The same CHO cell lines in (A) were transfected with increasing amounts of plasmids encoding NPC2-myc or β-gal (0.5ug–2ug). (C) Conditioned media from CHO-Vector and CHO-NgBR transfected with NPC2-myc was collected and NPC2-myc was immunoprecipitated from the media using anti-myc antibodies. (D) Pulse-Chase analysis of NPC2. CHO cell lines were transfected with NPC2-myc and subjected to ^{35}S-Met/Cys incorporation for half-life determination of NPC2 in the absence and presence of NgBR expression. Error bars represent the ± S.E. of pooled data from 3 independent experiments. (E) NgBR knockdown and NPC2 levels. HepG2 and EA.hy926 cells were incubated with RNAi directed against NgBR for 48 hours. Cells were lysed and lysates were blotted for endogenous NgBR, NPC2, and Cathepsin D. (F) Analysis of NPC2 degradation. NgBR knockdown was performed as in (E) in the absence or presence of proteasome inhibitor (MG132, 5μM, 24hrs; or lactacystin, 5μM, 24hrs). After 48hrs of RNAi treatment, cells were lysed and lysates blotted for endogenous NgBR, NPC2, and Cathepsin D.

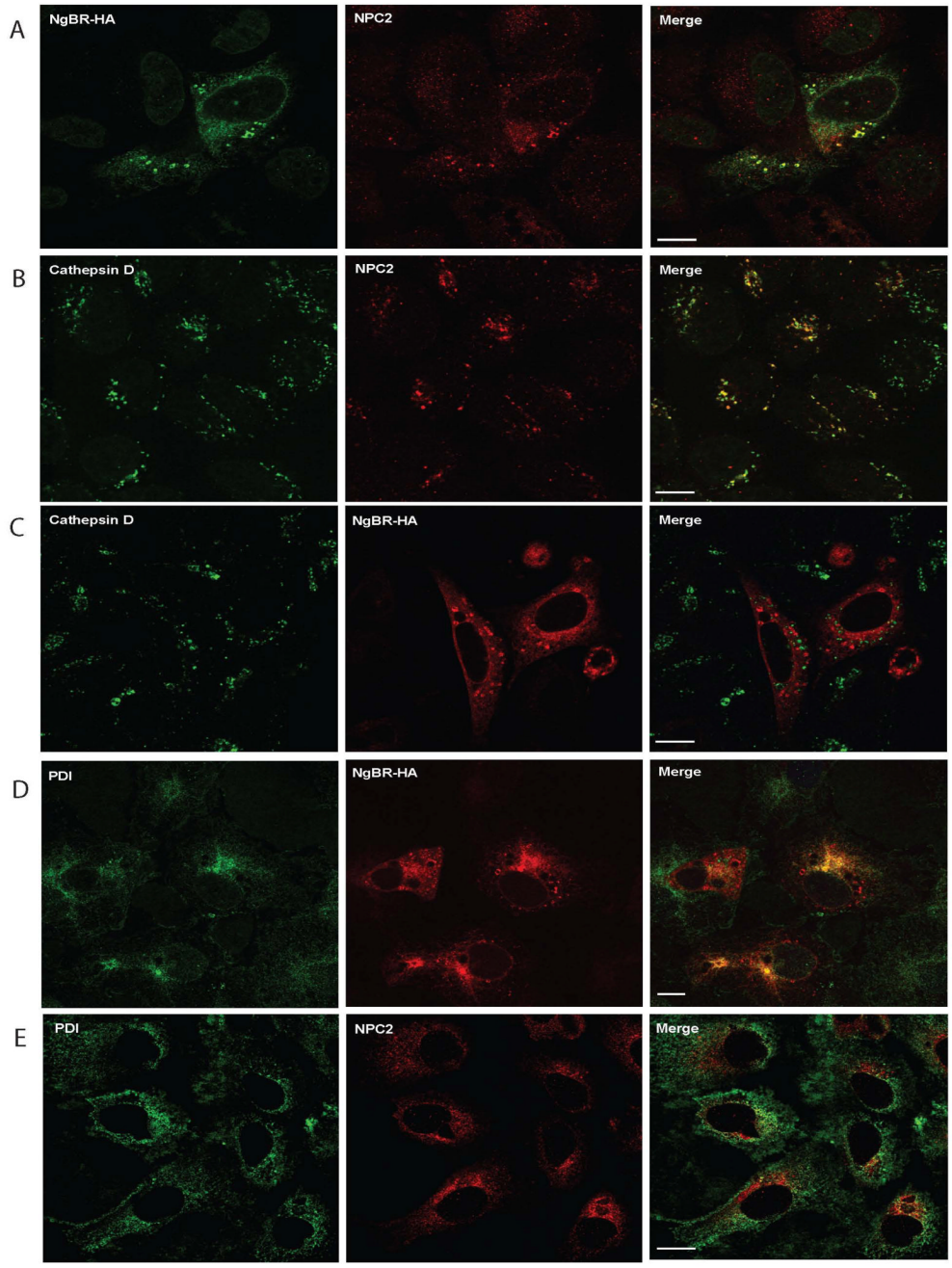

Figure 2. Evidence supporting localization of NgBR and NPC2 in a pre-lysosomal Compartment

(A–E) HeLa cells transfected with NgBR-HA were fixed and stained with antibodies against HA, NPC2, Cathepsin D, and PDI using Bouin's fixative for detection of endogenous NPC2 (scale bar = 10μm).

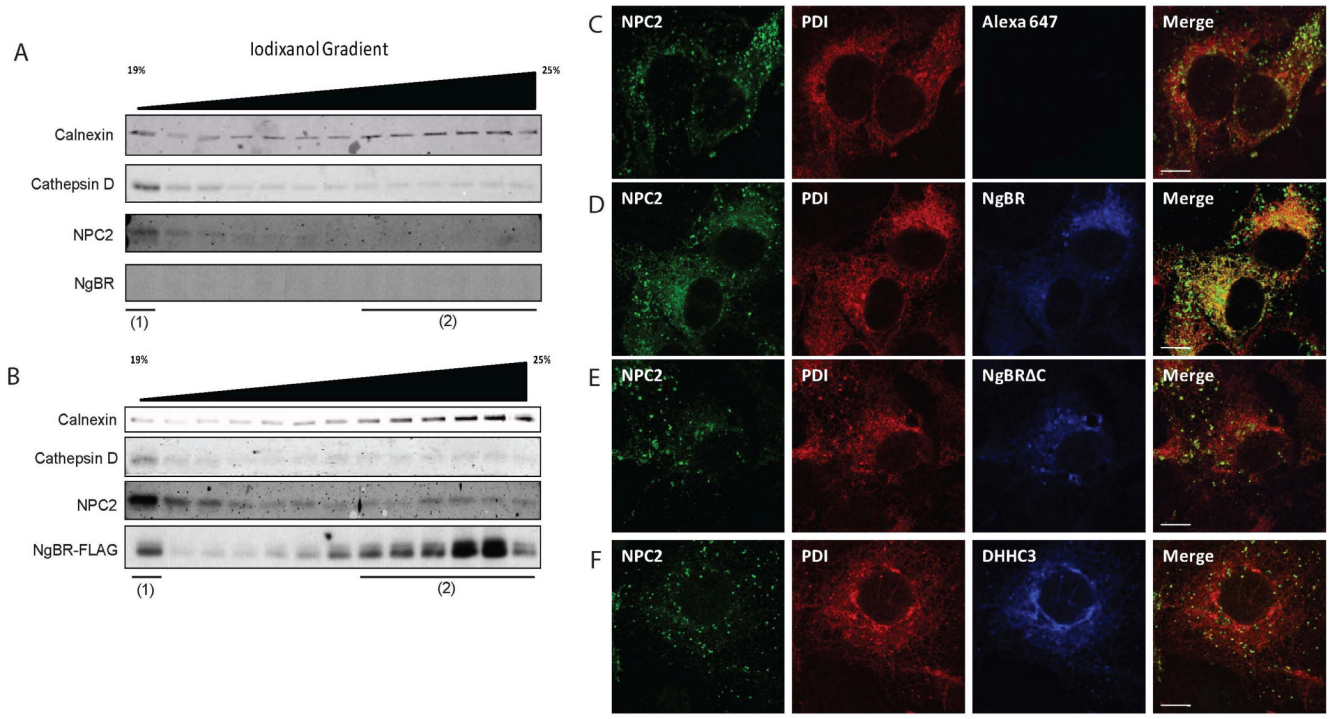

Figure 3.

(A,B) ER membrane fractionation with iodixanol was performed as described by Radhakrishnan et al (see Supplementary Experimental Procedures). ER vs. lysosomal localization was assessed by fractionation of HEK-293T cells over an iodixanol gradient. Cells in (A) contain endogenous levels of NPC2 and NgBR; cells in (B) contain endogenous NPC2 but overexpressed NgBR. Fraction (1) is defined as a mixture of lysosomes, peroxisomes, and ER, and Fraction (2) is defined as purified ER (Radhakrishnan et al., 2008). (C–F) COS cells transfected with control plasmid (C), WT NgBR-HA (D), NgBRΔC-HA (E), or DHHC3-HA (F) were fixed with Bouin's fixative and stained with anti-NPC2, anti-PDI, and anti-HA antibodies followed by secondary antibodies as described in Experimental Procedures (scale bar = 10μm).

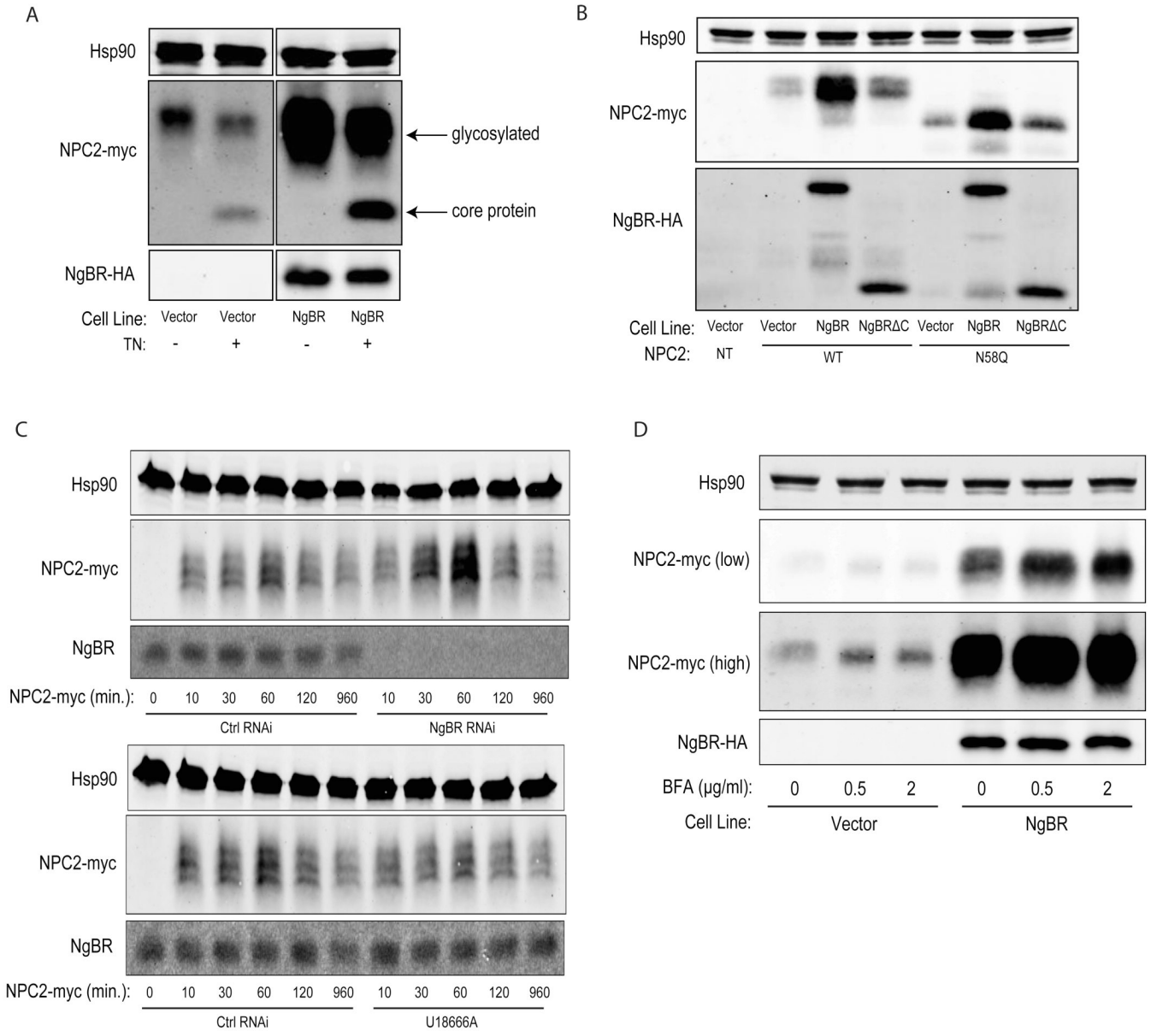

Figure 4.

(A) CHO cell lines (see Fig. 1D) were transfected with NPC2, incubated for 24 hours followed by treatment with 5ug/ml tunicamycin (TN) for 6 hours. (B) WT NPC2-myc or NPC2^{N58Q}myc was transfected into CHO cell lines and levels of NPC2-myc assessed by Western blotting. (C) After 48hrs of treatment with Ctrl RNAi or RNAi directed against NgBR, EA.hy cells were treated for the indicated times with 1% (final concentration, vol/vol) concentrated conditioned medium from CHO cells transfected with NPC2-myc. A subset of Ctrl RNAi-treated cells were pre-treated with U18666A (1μM, 8hrs) prior to addition of exogenous NPC2. (D) CHO cells stably expressing a Vector control (Vector) or full-length NgBR (NgBR) were transfected with myc-tagged NPC2. 24hrs post-transfection, cells were treated with the indicated amounts of brefeldin A for 8hrs, lysed, and immunoblotting was performed for detection of NPC2 levels.

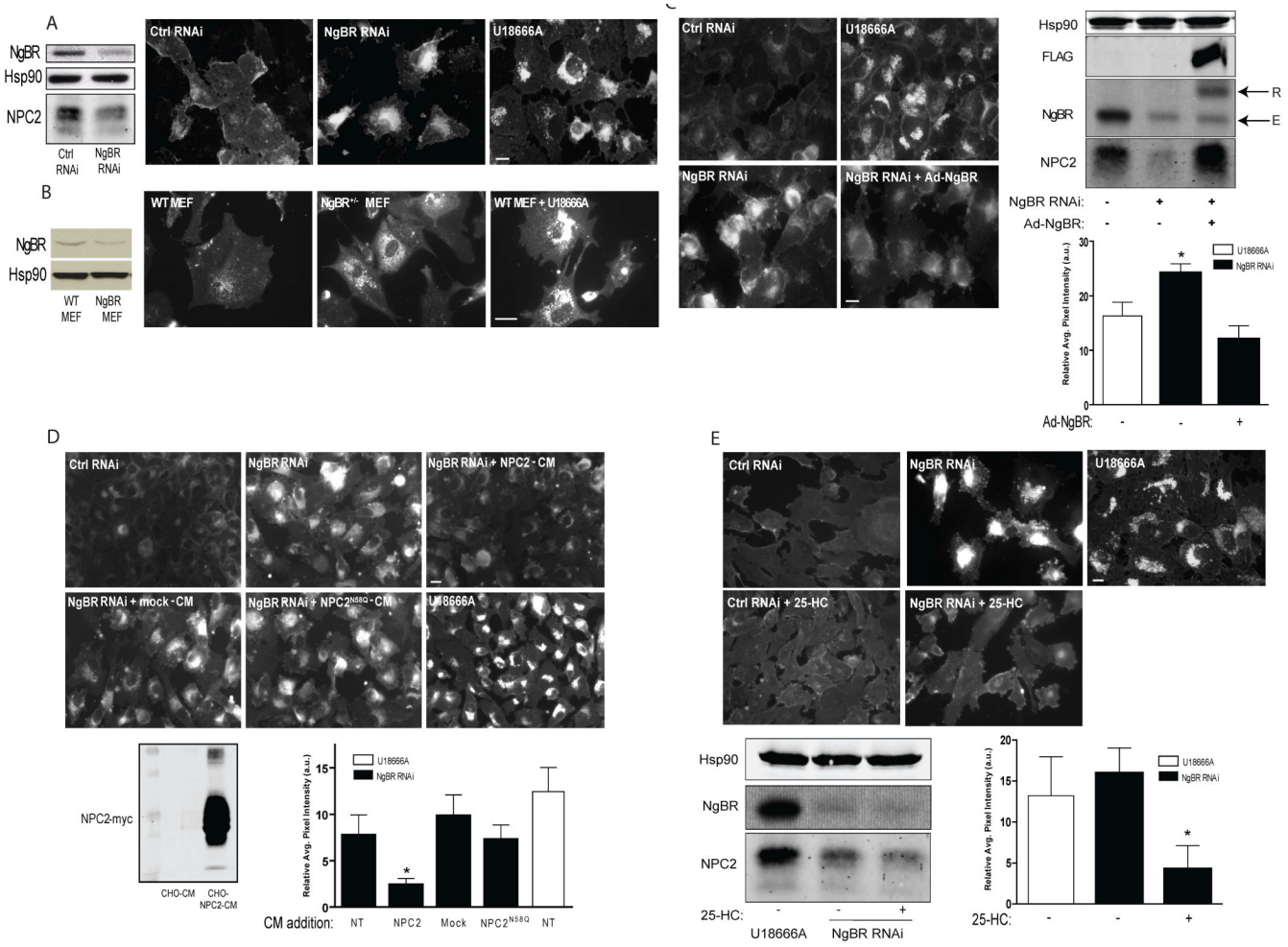

Figure 5. Loss of NgBR induces free cholesterol accumulation in cells

(A) EA.hy926 cells or (B) NgBR$^{+/-}$ fibroblasts (MEFs) were incubated with non-silencing RNA (Ctrl RNAi) or small interfering RNA directed against NgBR (NgBR RNAi) for 48 hours. U18666A (1μM, 8hours) was used as a positive control for inhibition of cholesterol trafficking. Cells were fixed and stained for free cholesterol with filipin as described in Experimental Procedures (scale bar = 20μm). (C) EA.hy926 cells were infected with an adenoviral construct expressing GFP or with adenovirus encoding NgBR (Ad-NgBR) for 24 hours, followed by incubation with Ctrl RNAi or NgBR RNAi for 48 hours. Cells were then fixed and stained for free cholesterol as in (A–B). (D) Conditioned medium from CHO cells transfected with NPC2-myc was concentrated and added to EA.hy926 cells incubated with Ctrl RNAi or NgBR RNAi for 24 hours. (E) EA.hy926 cells treated with Ctrl RNAi or NgBR RNAi were incubated with 2.5μM 25-hydroxycholesterol (25-HC) for 18 hours followed by fixation and staining with filipin. (*$p < 0.05$).

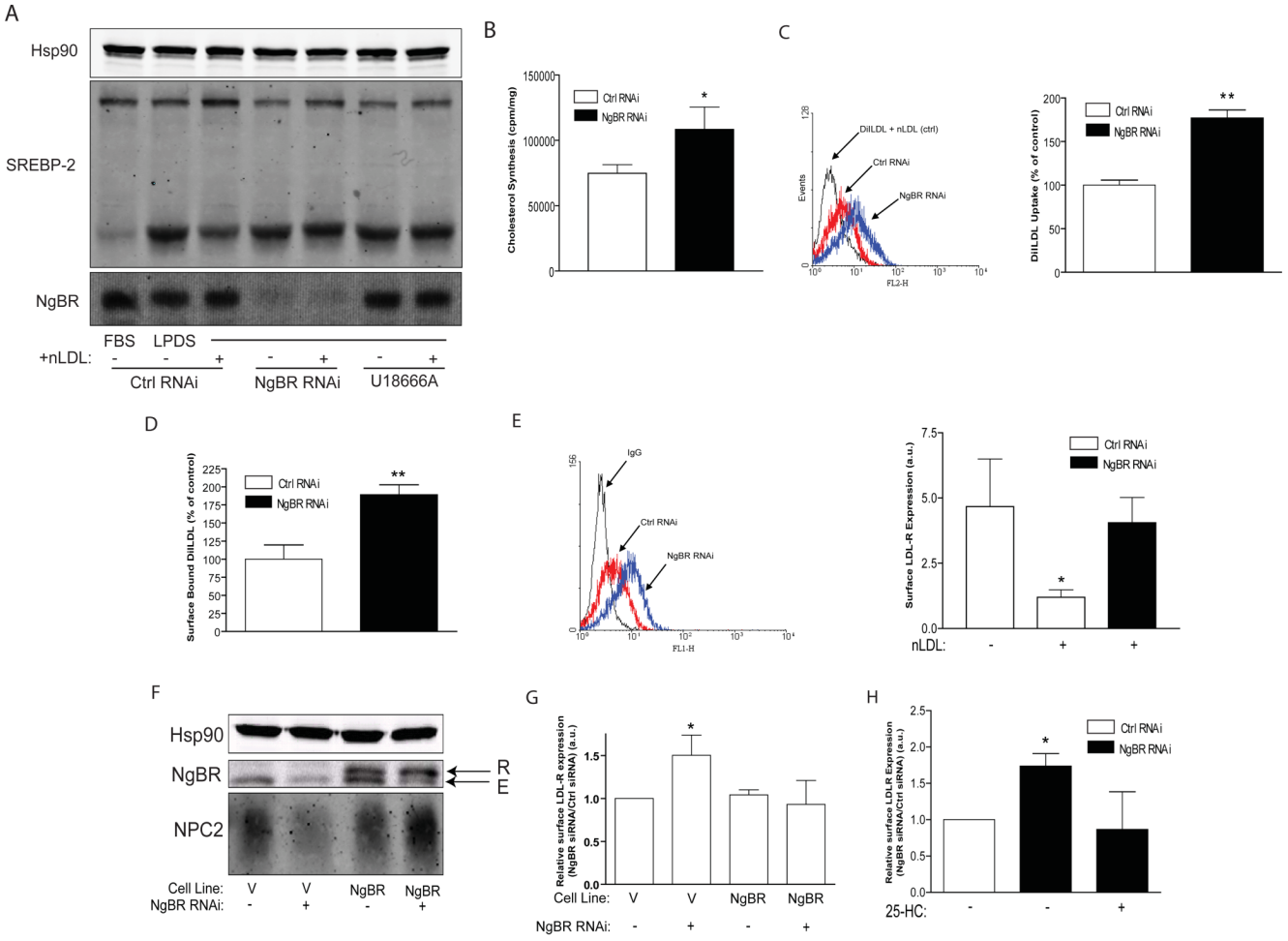

Figure 6. NgBR expression is necessary for proper regulation of cellular cholesterol Homeostasis

(A) SREBP-2 cleavage assay. EA.hy cells were treated with Ctrl RNAi or NgBR RNAi for 12hrs followed by addition of FBS or lipoprotein-deficient serum (LPDS) for a further 48hrs. Cells either remained in LPDS or were treated with 20μg/ml nLDL for 10hrs prior to lysis. (B) Cholesterol biosynthesis in HepG2 cells. HepG2 were treated with Ctrl RNAi or NgBR RNAi for 48 hours. Cholesterol biosynthesis was examined as described in Experimental Procedures. (C–D) EA.hy926 cells were treated with Ctrl RNAi or NgBR RNAi and LDL uptake and surface LDL binding measurements were performed as described in Experimental Procedures. (E) EA.hy926 cells treated with Ctrl RNAi or NgBR RNAi were subjected to analysis of LDL-R expression as described in Experimental Procedures. (F) HepG2 cell line stably expressing full-length NgBR. Ctrl RNAi or NgBR RNAi was incubated with HepG2 cells stably expressing either empty vector (V) or an RNAi-resistant NgBR construct (NGBR). (G) Surface LDL-R expression was analyzed in HepG2 stable cell lines after treatment with NgBR RNAi as described in Experimental Procedures. (H) EA.hy926 cells were treated with RNAi for 24 hours, followed by incubation with lipoprotein-deficient serum supplemented with nLDL in the absence or presence of 2.5μM 25-hydroxycholesterol (25-HC) for 24 hours. Surface LDL-R expression (H) was analyzed by flow cytometry as described in Experimental Procedures. (*$p < 0.05$, **$p < 0.01$).